(Received 20 December 2024, Accepted 26 February 2025, Scheduled 17 March 2025)

Novel Construction of Characteristic Basis Functions Accelerated Multilevel Characteristic Basis Function Method for Fast Solution of Electrically Large Scattering Problems

Mingrui Ou[1], Yufa Sun[1], Ling Yao[2,*], and Pan Wang[1]

[1] School of Electronic and Information Engineering, Anhui University, Hefei 230601, China
[2] School of Electronic Engineering, Anhui Xinhua University, Hefei 230088, China

ABSTRACT: In this paper, a novel construction approach of characteristic basis functions (CBFs) is proposed to accelerate the traditional multilevel characteristic basis function method (MLCBFM) for the analysis of electrically large scattering problems. The solution of CBFs in the traditional MLCBFM is extremely complicated and time-consuming due to numerous reduced matrix calculation procedures. Nevertheless, in the proposed method, the CBFs can be solved directly in one step using the new construction approach, which leads to a significant reduction in computation time. Numerical simulation results have demonstrated the effectiveness of the proposed method, which achieves higher computational efficiency without any loss of accuracy than the traditional MLCBFM.

1. INTRODUCTION

The method of moments (MoM) [1] is an effective numerical approach for analyzing electromagnetic scattering problems, which has strong adaptability and high accuracy. However, as the number of unknowns increases, the solution of the dense matrix constructed by the MoM becomes very difficult. To address this issue, many researchers have proposed various innovative approaches, such as wavelet MoM [2], multilevel fast multipole algorithm (MLFMA) [3], adaptive integral method [4], and characteristic basis function method (CBFM) [5–7]. By reducing the dimension of the matrix or speeding up the filling of the matrix elements, these methods have achieved considerable success. Among these methods, CBFM uses the idea of partitioning to divide the target into subdomains and solve the unknown current on each subdomain separately. By the division of subdomains, the dimension of the matrix equation on each subdomain is greatly reduced. Thus, the calculation efficiency is improved. Additionally, the CBFM based on singular value decomposition (SVD) [8, 9] was proposed to construct a new set of characteristic basis functions (CBFs) independent of polarization and angles, which is suitable to deal with multiple excitation problems. Based on SVD-CBFM, an ultra-wideband CBFM (UCBFM) [10–12] is presented to analyze broadband scattering problems. Nevertheless, when the number of unknowns within the subdomain is still large, solving the matrix equation on the subdomain is still time-consuming. To overcome this problem, multilevel characteristic basis function method (MLCBFM) [13] divides each subdomain into smaller subdomains through multilevel division. The CBFs defined on each higher-level subdomain can be represented by the linear combination of the CBFs on the lower-level subdomains, and the total current can be similarly obtained by the CBFs defined on the top-level subdomains. Although MLCBFM has achieved good performance, as the number of subdomains increases, the generation of CBFs will be time-consuming.

To accelerate MLCBFM, some fast algorithms have been introduced to MLCBFM. Adaptive cross approximation (ACA) [14, 15] is combined with MLCBFM to accelerate the calculation of the reduced matrix. A hybrid approach [16] is presented by combining ACA and fast dipole method (FDM) with MLCBFM to accelerate the calculations of impedance and reduced matrices. To accelerate the calculation of CBFs, a large-size blocks-based MLCBFM is presented in [17], and the multiscale compressed block decomposition [18] is combined with MLCBFM. A fast algorithm for the calculation of far interactions in MLCBFM is proposed in [19]. MLFMA [20] is implemented with MLCBFM to accelerate the calculations of higher-level impedance matrices from lower-level ones. In [21], the MLCBFM based on PMCHWT formulation is proposed for solving electromagnetic characteristics from multi-dielectric and perfect electrical conductor (PEC) composite objects. Recently, compressive sensing (CS) [22] technology has been introduced into MLCBFM to replace the solution of reduced matrix. These studies accelerated the computation process of MLCBFM from different aspects, and all of them have yielded good results.

Unlike previous works, we present a novel construction approach of CBFs with MLCBFM, which is based on the Foldy-Lax multiple scattering equation to improve the efficiency of generating CBFs. In the proposed method, the primary CBF (PCBF) is generated only by the original excitation, while the secondary CBFs (SCBFs) are generated by the scattering of

* Corresponding author: Ling Yao (yl_9920@sina.com).

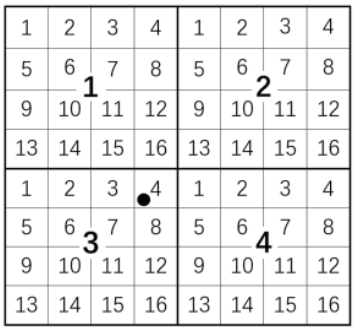

FIGURE 1. Multilevel division of objects.

all other upper-level subdomains and other same-level subdomains within the same upper-level subdomain. For all other higher levels, their CBFs can be obtained directly by combining their lower-level ones. With this new construction approach of CBFs, the solution time of CBFs is greatly reduced, while the computational accuracy is maintained after taking the appropriate order of SCBFs compared to MLCBFM. The results of numerical simulations have validated the effectiveness of the proposed method.

2. THEORY

2.1. Traditional MLCBFM

CBFM has achieved remarkable success in reducing the dimension of matrix equations, whereas, as the electrical size of the target increases, this efficiency advantage becomes less and less obvious. The creation of MLCBFM is precisely to address this problem. According to MLCBFM, m subdomains are obtained by first dividing the surface of the object, and then each large subdomain is further divided into n smaller ones. By analogy, we can get different levels of subdomains as needed, and the bottom subdomains are split with RWG basis functions [23]. As shown in Fig. 1, we divide the object into two levels, generating four ($m = 4$) first-level and 16 ($n = 16$) second-level subdomains in each first-level subdomain. The black dot denotes the 4th small subdomain in the 3rd large subdomain, which is denoted by the symbol $3\{4\}$. The process of expanding from low-level subdomains to high-level ones is illustrated in Fig. 2. Supposing that we calculate SCBFs to the second order on each level, then the solving process of the induced current is as follows:

2.1.1. Generation of PCBF

In the calculation of PCBF, both the effect of original excitation and the interactions of other small subdomains in the same large subdomain are considered. As shown in Fig. 3(a), apart from the incident excitation, the interactions from subdomains colored in yellow are considered when calculating the PCBF of subdomain $3\{7\}$. The specific solution procedure is as follows:

$$\mathbf{Z}_{i\{k\}i\{k\}}\mathbf{J}_{i\{k\}}^{(2)PP} = \mathbf{E}_{i\{k\}} \tag{1}$$

$$\mathbf{Z}_{i\{k\}i\{k\}}\mathbf{J}_{i\{k\}}^{(2)PS_1} = -\sum\nolimits_{h=1(h\neq k)}^{n} \mathbf{Z}_{i\{k\}i\{h\}}\mathbf{J}_{i\{h\}}^{(2)PP} \tag{2}$$

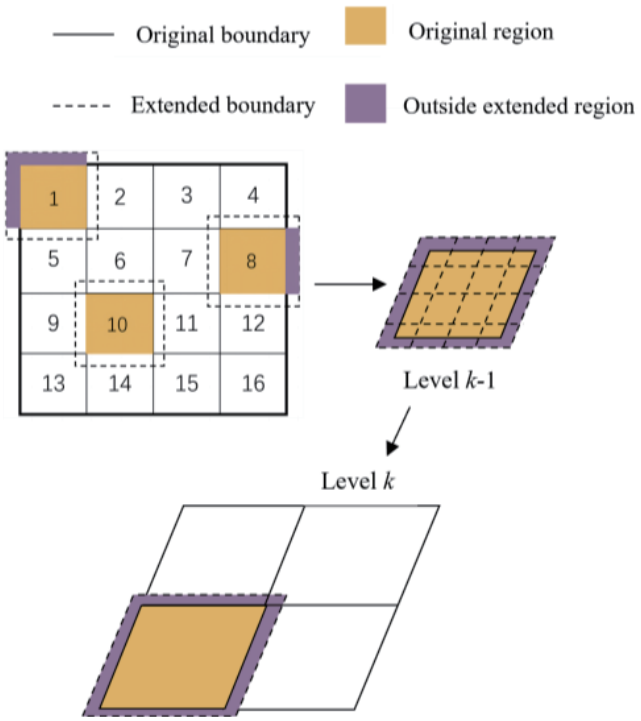

FIGURE 2. The generation of high-level subdomains.

$$\mathbf{Z}_{i\{k\}i\{k\}}\mathbf{J}_{i\{k\}}^{(2)PS_2} = -\sum\nolimits_{h=1(h\neq k)}^{n} \mathbf{Z}_{i\{k\}i\{h\}}\mathbf{J}_{i\{h\}}^{(2)PS_1} \tag{3}$$

$$\mathbf{J}_{i\{k\}}^{(2)P} = a_{i\{k\}}^{(2)P}\mathbf{J}_{i\{k\}}^{(2)PP} + b_{i\{k\}}^{(2)P}\mathbf{J}_{i\{k\}}^{(2)PS_1} + c_{i\{k\}}^{(2)P}\mathbf{J}_{i\{k\}}^{(2)PS_2} \tag{4}$$

$$\mathbf{J}_{i}^{(1)P} = \left[\mathbf{J}_{i\{1\}}^{(2)P}, \mathbf{J}_{i\{2\}}^{(2)P}, \ldots, \mathbf{J}_{i\{n\}}^{(2)P}\right]^{T} \tag{5}$$

where $i = 1, \ldots, m$; $k, h = 1, \ldots, n$; $\mathbf{J}_{i}^{(1)P}$ is the first-level PCBF; and $\mathbf{J}_{i\{k\}}^{(2)P}$ is the second-level (bottom-level) PCBF, while $\mathbf{J}_{i\{k\}}^{(2)PP}$, $\mathbf{J}_{i\{k\}}^{(2)PS_1}$ and $\mathbf{J}_{i\{k\}}^{(2)PS_2}$ are the CBFs of $\mathbf{J}_{i\{k\}}^{(2)P}$; $a_{i\{k\}}^{(2)P}$, $b_{i\{k\}}^{(2)P}$, and $c_{i\{k\}}^{(2)P}$ are the coefficients and the impedance matrix between the kth and hth subdomains in the same ith upper-level subdomain is represented by $\mathbf{Z}_{i\{k\}i\{h\}}$, while the excitation vector is represented by $\mathbf{E}_{i\{k\}}$.

2.1.2. Generation of SCBFs

Unlike the calculation of PCBF, the calculations of SCBFs consider the interactions of other subdomains on the same level as illustrated in Fig. 3(b). The first-order SCBFs are calculated as follows:

$$\mathbf{Z}_{i\{k\}i\{k\}}\mathbf{J}_{i\{k\}}^{(2)S_1P} = -\sum\nolimits_{j=1(j\neq i)}^{m} \mathbf{Z}_{i\{k\}j}\mathbf{J}_{j}^{(1)P} \tag{6}$$

$$\mathbf{Z}_{i\{k\}i\{k\}}\mathbf{J}_{i\{k\}}^{(2)S_1S_1} = -\sum\nolimits_{h=1(h\neq k)}^{n} \mathbf{Z}_{i\{k\}i\{h\}}\mathbf{J}_{i\{h\}}^{(2)S_1P} \tag{7}$$

$$\mathbf{Z}_{i\{k\}i\{k\}}\mathbf{J}_{i\{k\}}^{(2)S_1S_2} = -\sum\nolimits_{h=1(h\neq k)}^{n} \mathbf{Z}_{i\{k\}i\{h\}}\mathbf{J}_{i\{h\}}^{(2)S_1S_1} \tag{8}$$

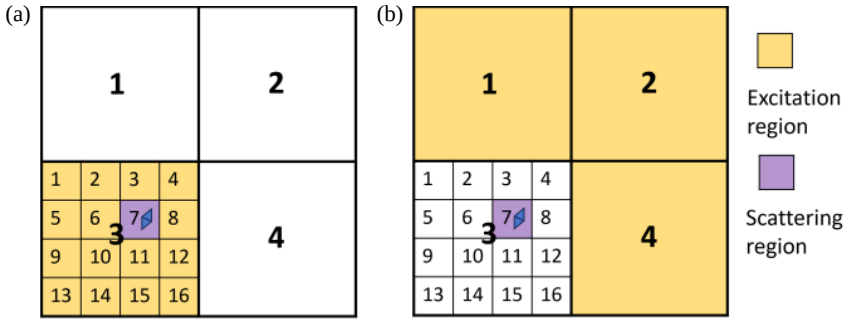

FIGURE 3. Interactions between subdomains with traditional MLCBFM. (a) PCBF. (b) SCBFs.

$$\mathbf{J}_{i\{k\}}^{(2)S_1} = a_{i\{k\}}^{(2)S_1}\mathbf{J}_{i\{k\}}^{(2)S_1P} + b_{i\{k\}}^{(2)S_1}\mathbf{J}_{i\{k\}}^{(2)S_1S_1} + c_{i\{k\}}^{(2)S_1}\mathbf{J}_{i\{k\}}^{(2)S_1S_2} \quad (9)$$

$$\mathbf{J}_i^{(1)S_1} = \left[\mathbf{J}_{i\{1\}}^{(2)S_1}\ \mathbf{J}_{i\{2\}}^{(2)S_1}\ \cdots\ \mathbf{J}_{i\{n\}}^{(2)S_1}\right]^T \quad (10)$$

where the impedance matrix between the kth subdomain in the ith upper-level subdomain and the jth upper-level subdomain is represented by $\mathbf{Z}_{i\{k\}j}$; $\mathbf{J}_{i\{k\}}^{(2)S_1}$ is the first-order SCBF on the second level, while $\mathbf{J}_{i\{k\}}^{(2)S_1P}$, $\mathbf{J}_{i\{k\}}^{(2)S_1S_1}$ and $\mathbf{J}_{i\{k\}}^{(2)S_1S_2}$ are the CBFs of $\mathbf{J}_{i\{k\}}^{(2)S_1}$; $a_{i\{k\}}^{(2)S_1}$, $b_{i\{k\}}^{(2)S_1}$ and $c_{i\{k\}}^{(2)S_1}$ are the coefficients; $\mathbf{J}_i^{(1)S_1}$ is the first-order SCBF on the first level.

In analogy, the second-order SCBF is calculated through the following steps:

$$\mathbf{Z}_{i\{k\}i\{k\}}\mathbf{J}_{i\{k\}}^{(2)S_2P} = -\sum_{j=1(j\neq i)}^{m}\mathbf{Z}_{i\{k\}j}\mathbf{J}_j^{(1)S_1} \quad (11)$$

$$\mathbf{Z}_{i\{k\}i\{k\}}\mathbf{J}_{i\{k\}}^{(2)S_2S_1} = -\sum_{h=1(h\neq k)}^{n}\mathbf{Z}_{i\{k\}i\{h\}}\mathbf{J}_{i\{h\}}^{(2)S_2P} \quad (12)$$

$$\mathbf{Z}_{i\{k\}i\{k\}}\mathbf{J}_{i\{k\}}^{(2)S_2S_2} = -\sum_{h=1(h\neq k)}^{n}\mathbf{Z}_{i\{k\}i\{h\}}\mathbf{J}_{i\{h\}}^{(2)S_2S_1} \quad (13)$$

$$\mathbf{J}_{i\{k\}}^{(2)S_2} = a_{i\{k\}}^{(2)S_2}\mathbf{J}_{i\{k\}}^{(2)S_2P} + b_{i\{k\}}^{(2)S_2}\mathbf{J}_{i\{k\}}^{(2)S_2S_1} + c_{i\{k\}}^{(2)S_2}\mathbf{J}_{i\{k\}}^{(2)S_2S_2} \quad (14)$$

$$\mathbf{J}_i^{(1)S_2} = \left[\mathbf{J}_{i\{1\}}^{(2)S_2}\ \mathbf{J}_{i\{2\}}^{(2)S_2}\ \cdots\ \mathbf{J}_{i\{n\}}^{(2)S_2}\right]^T \quad (15)$$

where $\mathbf{J}_{i\{k\}}^{(2)S_2}$ is the second-order SCBF on the second level, while $\mathbf{J}_{i\{k\}}^{(2)S_2P}$, $\mathbf{J}_{i\{k\}}^{(2)S_2S_1}$ and $\mathbf{J}_{i\{k\}}^{(2)S_2S_2}$ are the CBFs of $\mathbf{J}_{i\{k\}}^{(2)S_2}$; $a_{i\{k\}}^{(2)S_2}$, $b_{i\{k\}}^{(2)S_2}$ and $c_{i\{k\}}^{(2)S_2}$ are the coefficients; $\mathbf{J}_i^{(1)S_2}$ is the second-order SCBF on the first level.

2.1.3. Solving the Total Currents

When we get the CBFs defined on the first-level subdomains, the total current is calculated as follows:

$$\mathbf{J}_i^{(1)} = a_i^{(1)}\mathbf{J}_i^{(1)P} + b_i^{(1)}\mathbf{J}_i^{(1)S_1} + c_i^{(1)}\mathbf{J}_i^{(1)S_2} \quad (16)$$

$$\mathbf{J} = \left[\mathbf{J}_1^{(1)}\ \mathbf{J}_2^{(1)}\ \cdots\ \mathbf{J}_m^{(1)}\right]^T \quad (17)$$

where $\mathbf{J}_i^{(1)}$ is the induced currents of ith subdomain on the first-level; $\mathbf{J}$ is the total induced currents; $a_i^{(1)}$, $b_i^{(1)}$, and $c_i^{(1)}$ are the coefficients. Then, the reduced matrix equation can be obtained by employing the Galerkin test method [24]. Eventually, we can obtain the coefficients $a_i^{(1)}$, $b_i^{(1)}$, and $c_i^{(1)}$ by solving the reduced matrix equation, and the total currents can be obtained as well.

2.2. Proposed Method

MLCBFM has further enhanced the computational efficiency for electrically large targets by multilevel division of subdomains. However, through the theoretical analysis of MLCBFM, one can see that the generation of CBFs is extremely complicated and time-consuming. Therefore, in this paper, a new construction approach of CBFs is presented to address this problem, through which the computational efficiency of PCBF and SCBFs is much improved. The comparison of the construction approach of PCBF between the proposed method and MLCBFM is illustrated in Fig. 4.

Similarly, SCBFs are constructed in the same way in the proposed method, whereas the right-hand excitation terms are different from MLCBFM when solving the lower CBFs. Specifically, the procedure for solving the induced currents using the proposed method is as follows.

2.2.1. Generation of PCBF

Different from MLCBFM, PCBF is now calculated by taking into account only the effect of the original excitation illustrated in Fig. 5(a). Equations for the computation of PCBF are as follows:

$$\mathbf{Z}_{i\{k\}i\{k\}}\mathbf{J}_{i\{k\}}^{(2)P} = \mathbf{E}_{i\{k\}} \quad (18)$$

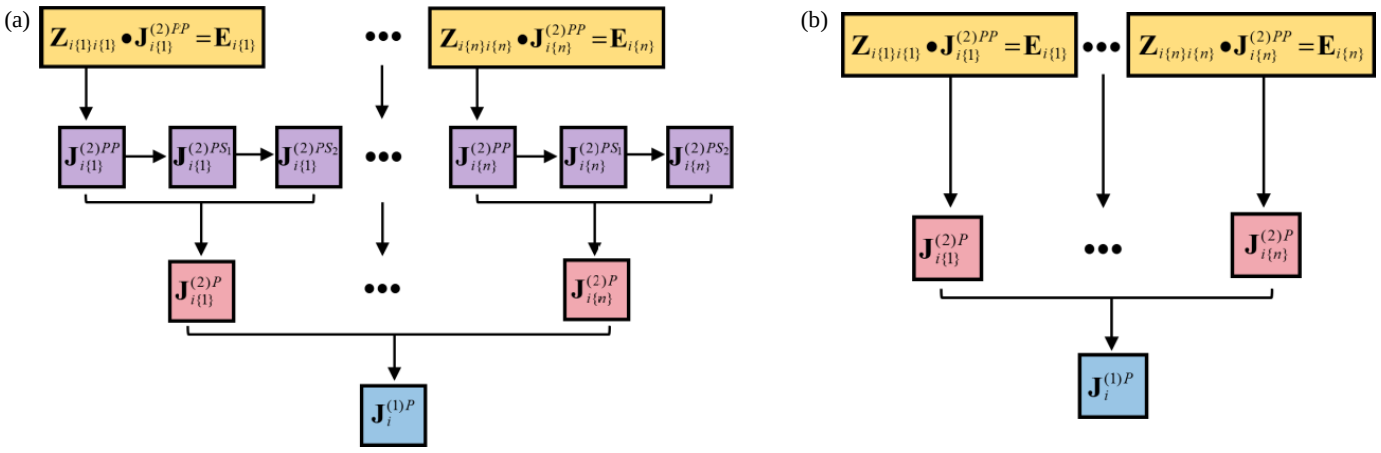

FIGURE 4. Comparison on construction approach of PCBF. (a) Traditional MLCBFM. (b) Proposed method.

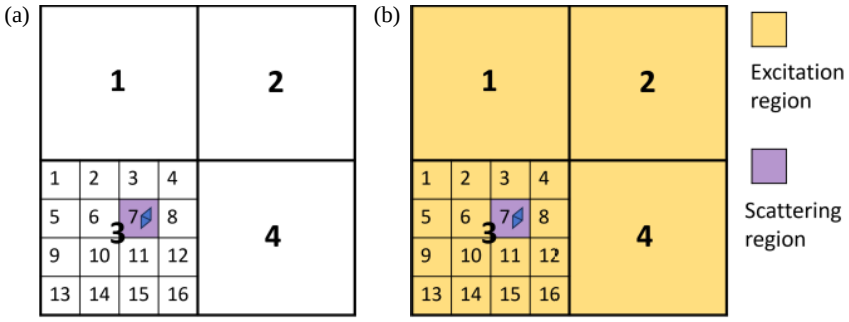

FIGURE 5. Interactions between subdomains with the proposed method. (a) PCBF. (b) SCBFs.

$$\mathbf{J}_i^{(1)P} = \left[\mathbf{J}_{i\{1\}}^{(2)P}\ \mathbf{J}_{i\{2\}}^{(2)P}\ \cdots\ \mathbf{J}_{i\{n\}}^{(2)P}\right]^T \tag{19}$$

One can see that the effects of other small subdomains within the same large subdomain are ignored here, which means that the calculations of Equations (2), (3), and (4) are avoided. However, we consider this part of the effects when solving SCBFs.

2.2.2. Generation of SCBFs

SCBFs are now calculated by considering not only the scattering effects of all other upper-level subdomains but also the interaction of other bottom-level subdomains in the same upper-level subdomain as shown in Fig. 5(b). The calculation of first-order SCBF is as follows:

$$\begin{aligned}\mathbf{Z}_{i\{k\}i\{k\}}\mathbf{J}_{i\{k\}}^{(2)S_1} &= -\sum\nolimits_{j=1(j\neq i)}^{m}\mathbf{Z}_{i\{k\}j}\mathbf{J}_j^{(1)P} \\ &\quad -\sum\nolimits_{h=1(h\neq k)}^{n}\mathbf{Z}_{i\{k\}i\{h\}}\mathbf{J}_{i\{h\}}^{(2)P}\end{aligned} \tag{20}$$

$$\mathbf{J}_i^{(1)S_1} = \left[\mathbf{J}_{i\{1\}}^{(2)S_1}\ \mathbf{J}_{i\{2\}}^{(2)S_1}\ \cdots\ \mathbf{J}_{i\{n\}}^{(2)S_1}\right]^T \tag{21}$$

The calculations of Equations (7), (8), and (9) are also avoided here due to the addition of the second item at the right side of Equation (20).

Likewise, we can also calculate the second-order SCBF as follows:

$$\begin{aligned}\mathbf{Z}_{i\{k\}i\{k\}}\mathbf{J}_{i\{k\}}^{(2)S_2} &= -\sum\nolimits_{j=1(j\neq i)}^{m}\mathbf{Z}_{i\{k\}j}\mathbf{J}_j^{(1)S_1} \\ &\quad -\sum\nolimits_{h=1(h\neq k)}^{n}\mathbf{Z}_{i\{k\}i\{h\}}\mathbf{J}_{i\{h\}}^{(2)S_1}\end{aligned} \tag{22}$$

$$\mathbf{J}_i^{(1)S_2} = \left[\mathbf{J}_{i\{1\}}^{(2)S_2}\ \mathbf{J}_{i\{2\}}^{(2)S_2}\ \cdots\ \mathbf{J}_{i\{n\}}^{(2)S_2}\right]^T \tag{23}$$

With the new construction approach of CBFs, the solution process of CBFs is greatly simplified, which greatly reduces computation time.

2.2.3. Solving the Total Currents

This step is the same with MLCBFM, and the total currents can be solved by Equations (16) and (17).

3. COMPLEXITY ANALYSIS

We compared the computational complexity between MLCBFM and the proposed method from two aspects: the calculation of PCBF and SCBFs. For the convenience of analysis, we still take a two-level subdomain division for example. Assuming that m large subdomains are divided, and n small subdomains are further divided in each of them, while N RWG functions are included in each small subdomain. The SCBFs on each level are considered to the kth order.

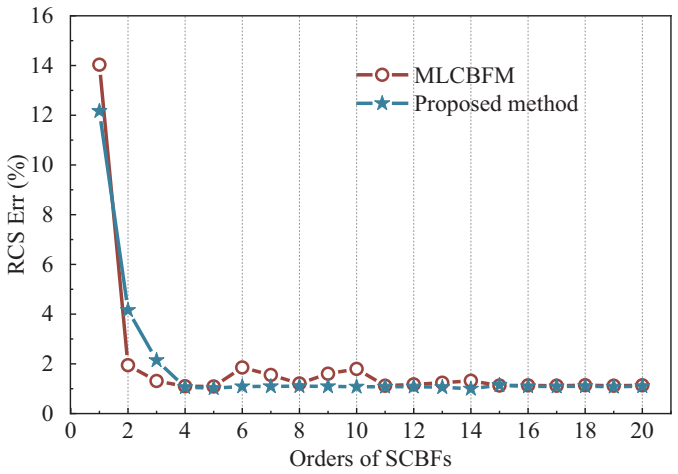

FIGURE 6. RCS Err versus different orders of SCBFs for the cuboid.

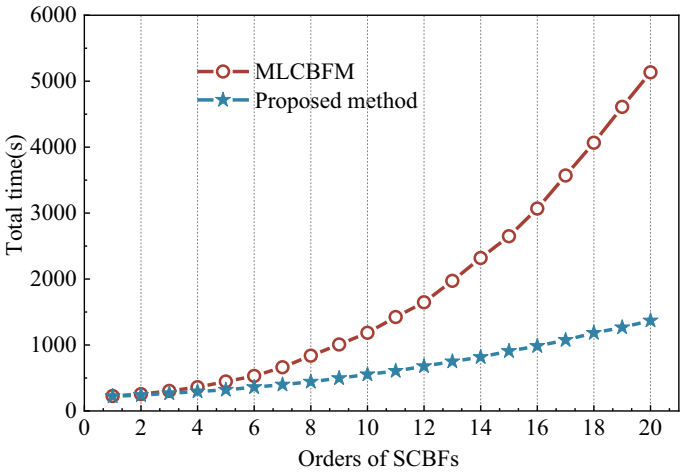

FIGURE 7. Total time versus different orders of SCBFs for the cuboid.

3.1. Calculation of PCBF

First, we take one of the large subdomains into consideration. In MLCBFM, the computational complexity for solving Equation (1) by lower-upper (LU) factorization is $O(nN^3)$, and the computational complexity for the solution of Equation (2) is $O(knN^2)$. The dimension of the reduced matrix is $(k+1)n\times(k+1)n$, and each element involves the calculation of $\mathbf{J}^T_{1\times N}\mathbf{Z}_{N\times N}\mathbf{J}_{N\times 1}$ whose computational complexity is $O(N^3)$. In addition, a computational complexity of $O((k+1)^3n^3)$ is also needed to solve the reduced matrix equation by LU factorization. Therefore, the computational complexity involved in a large subdomain is $O(nN^3+knN^2+(k+1)^2n^2N^3+(k+1)^3n^3)$. Considering all large subdomains, the total computational complexity for calculating PCBF with MLCBFM is $O(mnN^3+mknN^2+m(k+1)^2n^2N^3+m(k+1)^3n^3)$.

For the proposed method, the computational complexity involved in a large subdomain only includes the solution of Equation (19) whose computational complexity is $O(N^3)$. Therefore, the total computational complexity for calculating the PCBF with the proposed method is $O(mnN^3)$, which is much smaller than that of the MLCBFM.

3.2. Calculation of SCBFs

Likewise, we can analyze the computational complexity for generating SCBFs in the same way. We also take one of the large subdomains into consideration at first. In MLCBFM, the generation of each order SCBF involves solutions like Equation (6) by LU factorization whose computational complexity is $O((k+1)nN^2)$. The construction and solution of the reduced matrix equation are similar to those of the PCBF, and the computational complexity is $O((k+1)^2n^2N^3)$ and $O((k+1)^3n^3)$, respectively. Therefore, considering all large subdomains, the total computational complexity for calculating SCBFs with MLCBFM is $O(mk(k+1)nN^2+mk(k+1)^2n^2N^3+mk(k+1)^3n^3)$.

For the proposed method, the computational complexity involved in a large subdomain only includes the solution of Equation (20) whose computational complexity is $O(knN^2)$. Thus, the total computational complexity for calculating SCBFs with the proposed method is $O(mknN^2)$, which is significantly smaller than that of MLCBFM.

Through the above analysis, one can see that a much lower computational complexity is achieved by the proposed method, which makes a great improvement in computational efficiency compared to MLCBFM.

4. NUMERICAL RESULTS

To evaluate the performance of the proposed method, three different types of models are simulated by FEKO software (MoM solver), MLCBFM, and the proposed method, respectively. All tests were done on the same computer which is equipped with the Intel(R) Xeon(R) Platinum 8383C CPU @ 2.70 GHz and 64.0 GB RAM. For evaluating the accuracy, radar cross section (RCS) error is defined as follows:

$$\text{Err}=\left(\frac{\|\sigma_{\text{CAL}}-\sigma_{\text{REF}}\|_2}{\|\sigma_{\text{REF}}\|_2}\right)\times 100\% \tag{24}$$

where σ_{CAL} represents RCS calculation results of the proposed method or MLCBFM, while σ_{REF} represents those of the FEKO.

First, we simulated a $15\lambda\times 0.4\lambda\times 0.4\lambda$ PEC cuboid with the 300 MHz incident plane wave. All the subdomains need to be extended by 0.2λ on each level for ensuring the continuity of the induced currents. We use RWG basis functions to split the surface of the cuboid, which yields 10254 triangular cells, resulting in 15381 original unknowns and 16581 extended unknowns, with four subdomains on the first level and eight subdomains on the second level. The comparison of computational accuracy and time consumption between the proposed method and MLCBFM at different orders is illustrated in Fig. 6 and Fig. 7, respectively. It is clear to see that the computational accuracy of the proposed method is higher and more stable than the MLCBFM when the order of SCBFs is greater than 4, and the efficiency of the proposed method is improved significantly as the order of SCBFs increases. In subsequent calculations,

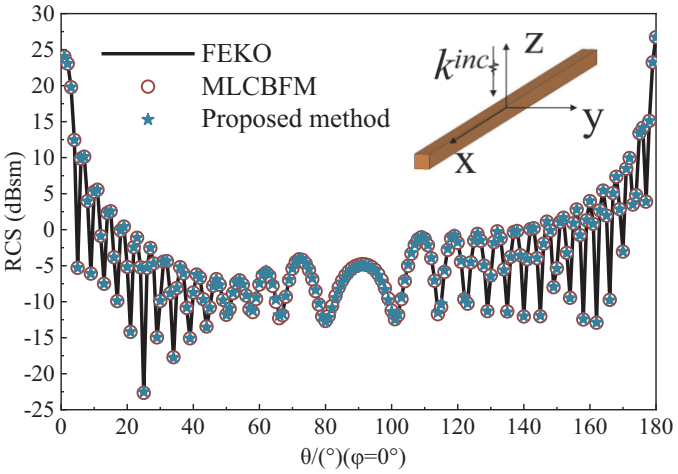

FIGURE 8. Bistatic RCS of the cuboid in H-polarization.

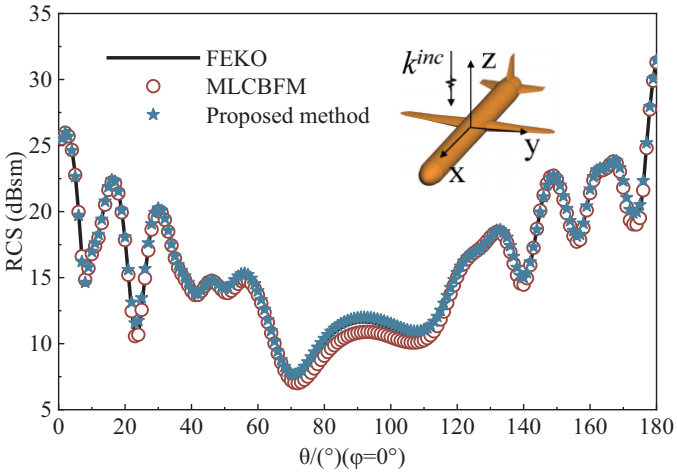

FIGURE 9. Bistatic RCS of the missile in H-polarization.

TABLE 1. Calculation time of three models using different methods.

Model	Method	Filling time (s)	CBFs time (s)	Solving time (s)	Total time (s)
Cuboid	MLCBFM	112.9	745.6	149.1	1007.6
	Proposed method	112.3	234.7	149.0	496.0
Missile	MLCBFM	514.6	1813.6	573.1	2901.3
	Proposed method	511.1	617.9	572.6	1701.6
Composite objects	MLCBFM	843.1	1307.1	2665.5	4810.3
	Proposed method	840.2	163.2	2663.1	3666.5

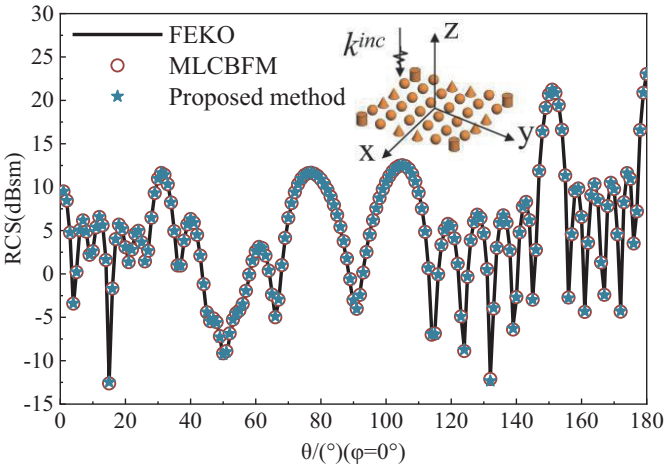

FIGURE 10. Bistatic RCS of composite objects in V-polarization.

SCBFs are considered to the 9th order on each level to obtain both stable and high accuracy. Simulation results of the H-polarized bistatic RCS of the cuboid are illustrated in Fig. 8. All the calculation results of the three methods are in good agreement.

Then, a PEC missile model with a length about 10λ is brought into consideration at 300 MHz. The missile is divided into 16880 triangular cells, resulting in 25320 original unknowns and 34827 extended unknowns with 0.2λ extended regions, which are split into eight first-level and 16 second-level subdomains, respectively. Bistatic RCS results of the missile model using different methods are displayed in Fig. 9, and the calculated results of the proposed method are closer to the FEKO results compared to those of the MLCBFM.

Last, the bistatic RCS of a composite target composed of 36 PEC objects in vertical polarization is calculated with the 2 GHz incident plane wave. The diameter and height of each object are λ, while the distance of every two adjacent objects is also λ. We divided the composite target into 29128 triangular cells, resulting in 43692 unknowns. With the two-level division strategy, nine subdomains are formed on the first level, while 36 subdomains are on the second level. As shown in Fig. 10, the results of both the proposed method and MLCBFM highly agree with those of the FEKO.

From Table 1, it is evident that the time consumption for the filling of the impedance matrix and the solution of the reduced matrix remains almost consistent between the proposed method and MLCBFM. However, the proposed method exhibits significantly improved efficiency for the generation of CBFs compared to the traditional MLCBFM due to the novel construction approach of CBFs, with reductions of computation time by 68.5%, 68.9%, and 87.5% for the three models, respectively. As a result, the total computation time of the three models using the proposed method is also significantly decreased compared to those using the traditional MLCBFM.

5. CONCLUSION

In this paper, we have presented a novel construction approach of CBFs to accelerate the conventional MLCBFM, through which the generation of CBFs becomes much simpler and faster. The solution process of CBFs with the conventional MLCBFM contains numerous reduced matrix calculations, which are comparatively complicated and require several steps to complete. However, with the new construction approach of CBFs, the solution of CBFs only needs one solving step, and the computational complexity is significantly reduced. The numerical simulations have validated that the proposed method exhibits higher computational efficiency than the traditional MLCBFM without any loss of accuracy.

ACKNOWLEDGEMENT

This work was supported by the National Natural Science Foundation of China under Grant No. 62071004.

REFERENCES

[1] Harrington, R. F., *Field Computation by Moment Methods*, IEEE Press, 1993.

[2] Vipiana, F., P. Pirinoli, and G. Vecchi, "Wavelet-MoM analysis of 3D antennas with triangular mesh," in *IEEE Antennas and Propagation Society Symposium, 2004*, Vol. 2, 1471–1474, Monterey, CA, USA, Jun. 2004.

[3] Song, J., C.-C. Lu, and W. C. Chew, "Multilevel fast multipole algorithm for electromagnetic scattering by large complex objects," *IEEE Transactions on Antennas and Propagation*, Vol. 45, No. 10, 1488–1493, Oct. 1997.

[4] Bleszynski, E., M. Bleszynski, and T. Jaroszewicz, "AIM: Adaptive integral method for solving large-scale electromagnetic scattering and radiation problems," *Radio Science*, Vol. 31, No. 5, 1225–1251, 1996.

[5] Prakash, V. V. S. and R. Mittra, "Characteristic basis function method: A new technique for efficient solution of method of moments matrix equations," *Microwave and Optical Technology Letters*, Vol. 36, No. 2, 95–100, 2003.

[6] Sun, Y. F., C. H. Chan, R. Mittra, and L. Tsang, "Characteristic basis function method for solving large problems arising in dense medium scattering," in *IEEE Antennas and Propagation Society International Symposium. Digest. Held in conjunction with: USNC/CNC/URSI North American Radio Sci. Meeting (Cat. No.03CH37450)*, Vol. 2, 1068–1071, Columbus, OH, USA, Jun. 2003.

[7] Wang, X., L. Chen, C. Liu, Y. Liu, Y. Zeng, and Z. Xu, "An efficient hybrid method of CBFM/AIM and equivalent dipole moment for computation of electromagnetic scattering problems," *IEEE Transactions on Antennas and Propagation*, Vol. 72, No. 10, 8103–8108, Oct. 2024.

[8] Lucente, E., A. Monorchio, and R. Mittra, "An iteration-free MoM approach based on excitation independent characteristic basis functions for solving large multiscale electromagnetic scattering problems," *IEEE Transactions on Antennas and Propagation*, Vol. 56, No. 4, 999–1007, Apr. 2008.

[9] Tanaka, T., K. Niino, and N. Nishimura, "Characteristic basis function method combined with krylov-calderón preconditioner for PMCHWT formulation," *IEEE Transactions on Antennas and Propagation*, Vol. 72, No. 3, 2578–2591, Mar. 2024.

[10] De Gregorio, M., G. Tiberi, A. Monorchio, and R. Mittra, "Solution of wide band scattering problems using the characteristic basis function method," *IET Microwaves, Antennas & Propagation*, Vol. 6, No. 1, 60–66, 2012.

[11] Nie, W.-Y. and Z.-G. Wang, "Solution for wide band scattering problems by using the improved ultra-wide band characteristic basis function method," *Progress In Electromagnetics Research Letters*, Vol. 58, 37–43, 2016.

[12] Wang, Z., C. Li, Y. Sun, W. Nie, P. Wang, and H. Lin, "A novel method for rapidly solving wideband RCS by combining UCBFM and compressive sensing," *Progress In Electromagnetics Research C*, Vol. 124, 33–42, 2022.

[13] Laviada, J., F. Las-Heras, M. R. Pino, and R. Mittra, "Solution of electrically large problems with multilevel characteristic basis functions," *IEEE Transactions on Antennas and Propagation*, Vol. 57, No. 10, 3189–3198, 2009.

[14] Chen, X., C. Gu, J. Ding, Z. Li, and Z. Niu, "Direct solution of electromagnetic scattering from perfect electric conducting targets using multilevel characteristic basis function method with adaptive cross approximation algorithm," *IET Microwaves, Antennas & Propagation*, Vol. 7, No. 3, 195–201, 2013.

[15] Li, C., Y. Sun, Z. Wang, and G. Wang, "Multilevel characteristic basis function method with ACA for accelerated solution of electrically large scattering problems," *Transactions of Nanjing University of Aeronautics and Astronautics*, Vol. 35, No. 3, 449–454, Jun. 2018.

[16] Li, C., Y. Sun, G. Wang, and Z. Wang, "Fast analysis for large-scale electromagnetic scattering problems by a hybrid approach," *Journal of Electromagnetic Waves and Applications*, Vol. 31, No. 8, 808–819, 2017.

[17] Huang, F. and Y. Sun, "Efficient solution of electromagnetic scattering from dielectric objects via characteristic basis function method based on large-size blocks with multilevel subdivision," *IEEE Access*, Vol. 7, 71 741–71 748, 2019.

[18] Fang, X., Q. Cao, and Y. Wang, "Accelerated direct solver with multiscale compressed block decomposition and multilevel characteristic basis function method," *IEEE Antennas and Wireless Propagation Letters*, Vol. 19, No. 12, 2226–2229, 2020.

[19] Park, C.-S., I.-P. Hong, I. Jung, and J.-G. Yook, "A fast computation of far interactions in MLCBFM for electromagnetic analysis of large structures," in *2018 International Symposium on Antennas and Propagation (ISAP)*, 1–2, Busan, Korea, Oct. 2018.

[20] Park, C.-S., I.-P. Hong, Y.-J. Kim, and J.-G. Yook, "Acceleration of multilevel characteristic basis function method by multilevel multipole approach," *IEEE Transactions on Antennas and Propagation*, Vol. 68, No. 10, 7109–7120, May 2020.

[21] Kim, I., H.-R. Im, Y. Ryu, I.-P. Hong, H. Lee, and J.-G. Yook, "Investigation on multilevel characteristic basis function method using PMCHWT formulation for multi-dielectric and PEC composite structures," in *2024 International Symposium on Antennas and Propagation (ISAP)*, 1–2, Incheon, Korea, Nov. 2024.

[22] Ou, M., Y. Sun, and C. Shi, "Compressive sensing enhanced multilevel characteristic basis function method for analyzing electrically large scattering problems," *IEEE Antennas and Wireless Propagation Letters*, Vol. 23, No. 2, 593–597, Feb. 2024.

[23] Rao, S., D. Wilton, and A. Glisson, "Electromagnetic scattering by surfaces of arbitrary shape," *IEEE Transactions on Antennas and Propagation*, Vol. 30, No. 3, 409–418, 1982.

[24] Galerkin, B. G., "On electrical circuits for the approximate solution of the Laplace equation," *Vestnik Inzh*, Vol. 19, 897–908, 1915.